

Helical Beams in Information Systems with Open Channels of Radiation Spread

A. V. Averchenko^a, A. M. Zotov^a, P. V. Korolenko^{a, b, *}, and N. N. Pavlov^{a, b}

^aFaculty of Physics, Moscow State University, Moscow, 119991 Russia

^bLebedev Physical Institute, Moscow, 119333 Russia

*e-mail: pvkorolenko@rambler.ru

Received July 29, 2019; revised August 30, 2019; accepted September 27, 2019

Abstract—The effectiveness of using light tubular beams with helical wave fronts in laser communication systems is considered, based on original methodological support and software. Negative effects arising from beam misalignment and turbulence in the medium of propagation are analyzed. A new way of improving the characteristics of helical laser fields is proposed.

DOI: 10.3103/S1062873820010050

INTRODUCTION

Studies aimed at improving optical communication systems based on open channels of radiation spread remain relevant today [1]. In recent years, attention has been given to the problem of transmitting information through the atmosphere using tubular beams with helical wave fronts. It has been emphasized in an number of works (e.g., [2] and [3–6]) that such helical beams are highly resistant to atmospheric turbulence. Despite the data on the properties of helical beams presented in the literature, some questions remain open. Among these are determining the effectiveness of beam multiplexing for a misaligned optical system, finding ways to increase the range of communication by generating powerful radiation with a helical phase surface, and developing algorithms and software for optimizing the characteristics of optical systems with open channels of radiation spread that have complex amplitudes and phase profiles. The aim of this work was to consider these problems.

ALGORITHM

The amplitude of the strength of the field in a helical beam is most often described by an expression that in a polar (r, φ, z) coordinate system takes the form [7]

$$E_l(r, \varphi) = \sqrt{\frac{2}{\pi(|l|)!}} \left[\frac{r\sqrt{2}}{w_0} \right]^{|l|} \frac{1}{w_0} \exp\left(\frac{-r^2}{w_0^2}\right) e^{il\varphi}. \quad (1)$$

Here, w_0 is the width of the beam in the neck when $z = 0$; l is the so-called topological charge of a helical field, which determines orbital phase advance ψ according to the formula $\psi = 2\pi l$. The width of a spreading beam grows and the wave front becomes

spherical. This transformation of the beam is described by the expressions

$$w^2(z) = w_0^2 \left[1 + \left(\frac{\lambda z}{\pi w_0^2} \right)^2 \right], \quad (2)$$

$$R(z) = z \left[1 + \left(\frac{\pi w_0^2}{\lambda z} \right)^2 \right], \quad (3)$$

where $w(z)$ and $R(z)$ are the beam width and the radius of curvature of the wave front at distance z from the neck, respectively, and λ is the wavelength.

At the first stage of this work, software allowing the determination of helical beam characteristics was developed along with elaborating questions of methodology. The need to develop special software was due to the large volume of calculations required for determining the parameters of laser radiation with a complex spatial structure under the action of random factors. Deriving the statistics of light wave fluctuation by averaging over many examples is a time-consuming process that lengthens the acquisition and processing of data considerably. We therefore decided to use the technology of parallel computation to speed up our calculations. In addition to parallel computations on a multicore central computer processor, calculations can be made on graphical processors. CUDA technology, which employs the PC video cards of graphical processors, was used in this work. Among other things, the CUDA platform for the quick processing of external functions in the MathCAD medium includes packages for linear algebra, fast Fourier transforms, and random number generators.

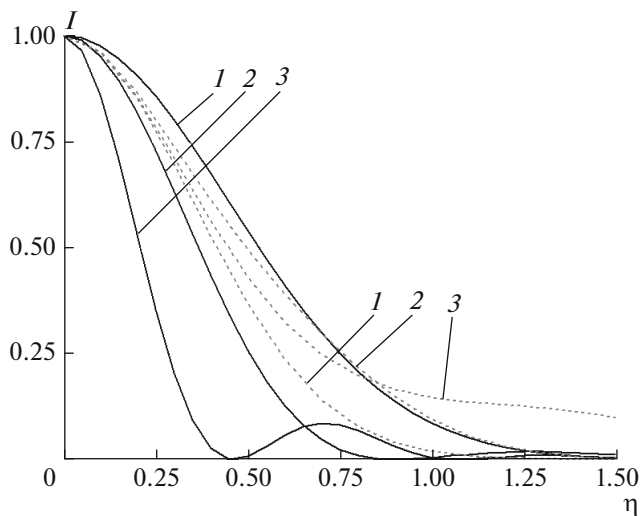


Fig. 1. Effect of misalignment parameter η on the drop in intensity I of waves with different l . (1) $l = 0$; (2) $l = 1$; (3) $l = 5$. The solid curves represent $\eta = \theta$, where θ is the angle of beam incidence, normalized to angle of divergence θ_0 of the main mode. The dashed line represents $\eta = \frac{\Delta x}{w_0}$, where Δx is the beam displacement.

If we have to monitor the power of a helical mode with index l passing through a phase screen and simulating a randomly inhomogeneous environment, it is sufficient to find the coefficient of coupling between perturbed and unperturbed modes. To calculate wave field \tilde{E}_l after it passes through the phase screen, which alters phase $f(x, y)$, we need only multiply amplitude E_l of a wave incident on the screen by factor $\exp(if(x, y))$:

$$\tilde{E}_l(x, y) = E_l(x, y) \exp(if(x, y)). \quad (4)$$

By determining the coefficient of coupling from the power between the indicated waves, we can find the power of the beam passing through the screen:

$$I_l = \left| \iint \tilde{E}_l(x, y) E_l^*(x, y) dx dy \right|^2. \quad (5)$$

The latter integral is taken over the entire working field. If the screen is random, then power I_l is determined according to its series of implementations.

When calculating the center of gravity of a beam at a certain distance from the initial plane, it is most efficient to decompose the field of a wave passing through the screen into plane waves. Plane waves travel a set distance without changing the module of amplitude, but those that spread at angle θ to axis z gain an additional phase progression. We can describe the diffraction spread of a field if we decompose it into plane waves, consider the phase progression for each of them, and fold them in given plane $z = L$.

Let us consider the spread of a beam in a given plane over area $a \times a$ with a homogeneous mesh of $N \times N$ points. Mesh step $d = a/N$ must be smaller than field irregularity D . The evolution of an individual beam must be studied at a sufficiently large a .

In a superpositioning of plane waves at distance L , we must consider that each of them has its own phase progression $\varphi_n = -2\pi L n^2 / T$, where n is the index ($n = 0, \pm 1, \pm 2, \dots$) of the wave spreading at angle $\theta_n = \lambda n / a$, and T is the so-called Talbot distance: $T = 2 \frac{a^2}{\lambda}$. Each complex wave amplitude with index n

must therefore be multiplied by $\exp\left(\frac{-i2\pi L n^2}{T}\right)$.

Decomposition into plane waves includes a number of subsequent operations: calculating the signal matrix, determining the spatial spectrum matrix using a 2D complex Fourier transform, multiplying the signal spectrum using a filter to determine the additional phase progressions of partial plane waves, and obtaining a signal matrix based on an inverse Fourier transform. We must also determine the dispersion of the center of gravity vibrations of the beam in addition to the field distribution at different points of the optical track. Since the main calculations were made in MathCAD medium, an individual user function based on CUDA in the form of a connectable dynamic library was written to determine the above parameters. In making our calculations, the initial parameters were wavelength λ , distance L along the optical track, and the discretization step of the considered distributions.

REQUIREMENTS FOR MULTIPLEXING HELICAL BEAMS

Since helical beams are widely used in communication systems with the multiplexing of spread channels, we investigated the effect beam misalignment has on the efficiency of these systems. The loss of beam power in particular was determined when angle of incidence θ on the receiving aperture was changed, and at parallel displacement Δx of its axis relative to that of the system. These losses can be estimated by determining the coefficient of coupling between misaligned and axial beams with corresponding charge l . Equation (5) can be used for this, assuming that parameter \tilde{E}_l characterizes the misaligned wave field.

Figure 1 shows the drop in power I of waves with different topological charges as the degree of misalignment grows. It is seen that at an angle of incidence one-tenth that of angle θ_0 of the misalignment of the main free space mode, the loss at l ranging from 0 to 5 rises from 5 to 20%. The losses also increase when the beam is displaced. Displacement equal to the half-radius of the main mode can therefore reduce registered power I by approximately 50%. Raising the topo-

logical charge can increase (by 5–10%) the loss of power as well. The curves in Fig. 1 testify to the need for careful alignment of the helical beams in multiplexing systems.

EFFECT OF ATMOSPHERIC INHOMOGENEITIES

An important factor affecting the losses of a helical beam is the turbulent atmosphere. The effect atmospheric inhomogeneities have on a beam was modeled using phase screens. The phase screen characteristics were chosen to correspond to atmospheric turbulence parameters of $C_n^2 = 10^{-14} - 10^{-16} \text{ cm}^{-2/3}$. The internal turbulence scale was $l_0 = 1 \text{ mm}$ and the external turbulence scale was $L_0 = 0.4 \text{ mm}$. The length of the atmospheric track was $L = 100 \text{ m}$. A modified von Karman spectrum of refractive index fluctuations (i.e., $\Phi^{\text{Ka}}(\kappa) = 0.033C_n^2(\kappa^2 + \kappa_0^2)^{-11/6} \exp(\kappa^2/\kappa_m^2)$) was used, where $\kappa_0 = 2\pi/L_0$, $\kappa_m = 5.92/l_0$. Parameter w_0 of the helical mode was 10 mm. The radiation wavelength was $\lambda = 500 \text{ nm}$.

The displacement of a phase screen in the direction perpendicular to a helical beam's axis induced random oscillations of its center of gravity at the end of the track. In our calculations, the effective transverse beam sizes with different l were assumed to be identical. Theoretical vibrations of the center of gravity of beams with $l = 0$ and $l = 3$ are shown in Fig. 2.

As is seen from the plots, the amplitude of displacement is higher for the main mode, since the wave front of the helical modes is strongly distorted by the narrower section of the phase screen.

Complementary calculations using modes with various l values confirmed the better stability of helical beams, relative to Gaussian modes of the same sizes.

USING MULTIBEAM RADIATION

Numerous attempts have been made to use multi-beam radiation for helical beam generation. Of special note is [8], which considered the possibility of forming helical beams based on a fiber laser matrix with a controlled phase.

The tubular behavior of helical beams indicates we can use spatial configurations of multipath modes (M-modes) as an alternative that ensures higher power. These modes are formed by light beams that, upon reflecting from the mirrors of a stable resonator beyond its optical axis, close the trajectory only after multiple reflections. M-mode generating beams thus have broken paths [7]. Each plane M-mode excited in a flat spherical resonator is characterized by index N , which denotes the number of double paths of a generating beam through a resonator. This index is uniquely

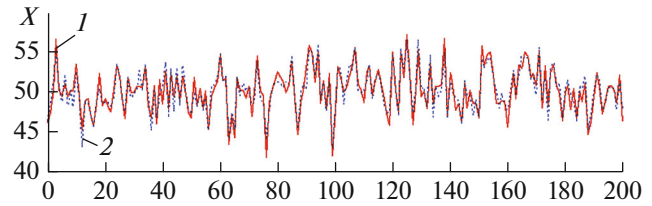


Fig. 2. Transverse displacement of light beams (in arbitrary units). The x-axis corresponds to the number of valuable points. (1) $l = 3$ (solid curve); (2) $l = 0$ (dashed line).

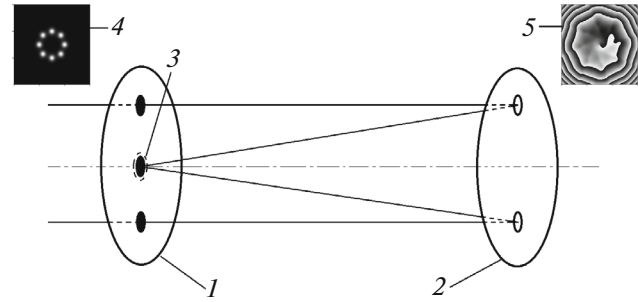


Fig. 3. Trajectories and light spots of a superposition of plane M-modes in a semi-confocal resonator: (1) flat mirror; (2) spherical mirror; (3) zone with the maximum coefficient of reflection; (4) arrangement of beams at the output of the laser; (5) wave front in the far zone.

determined by the geometrical parameters of the resonator:

$$\frac{1}{N} = \pi^{-1} \arccos \sqrt{1 - L/R}, \quad (6)$$

where L is the length of the resonator, and R is the radius of curvature of the spherical mirror. Figure 3 shows the trajectories and distributions of the light beams of plane M-modes excited in a semi-confocal resonator ($N = 4$). All M-modes are frequency degenerate, relative to the light beams on the mirrors. To obtain tubular beams, a system of modes with an azimuthal change of their plane must be excited in the laser resonator. Their energy output must come through beams parallel to the resonator axis. The maximum quality factor of the planar modes, relative to other types of resonator vibrations at simultaneous perturbations of the non-axial beam output, can be achieved by forming a small non-transparent zone with a high coefficient of reflection at the center of a flat mirror. A system of planar modes will form a system of light beams located around the circumference on the output mirror (see the inset 4 in Fig. 3). By choosing the radius of the nontransparent zone, we can achieve mode synchronization and the phasing of light vibrations in spots.

Since only parallel beams leave the resonator, the output radiation will have zero geometric divergence. At great distances from the output flat mirror, the field

distribution will be an intense central core with a system of peripheral diffraction rings (the same structure will also lie in the focal plane of a collecting lens in front of the receiver).

Attaching a piezoelectric head to the central non-transparent zone, which produces its fast low-amplitude longitudinal vibrations, we can obtain frequency modulation of the radiation by changing the length of the M-mode trajectory. Since the displacements of the central band will be smaller than the wavelength, these variations in length will not have a strong effect on the total intra-resonator field configuration. Using lasers operating on M-modes tuned to different frequencies, we can notably increase the volume of transmitted information. Beams can be bred on the receiver using a system of cascade Mach–Zander fiber interferometers. At a sufficiently large radius of the circumference with light spots, the output beam can be forced to pass through a long optical track with a considerable low-intensity near-axial zone. This will ensure its high stability when passing through the turbulent atmosphere. In practice, we must consider that the tubular configuration of a beam can be destroyed due to beam overlap as it spreads in space. Calculations using Eq. (2) showed that optimum track length z for M-modes as a function of output aperture diameter D obeys the law $z = 2.96 D$ when z and D are normalized to confocal parameter $z_0 = kw_0^2$, where k is the wave number and w_0 is the minimum radius of the generating beam.

A zone with zero intensity on its axis can be additionally expanded if opposite spots on its circumference are out of phase, forming a singular field in the interference. Spots out of phase can be obtained by locally reducing the coefficient of reflection at the center of a nontransparent zone. The output radiation in the far zone will have a helical wave front, as is seen from the hologram in inset 5 of Fig. 3.

CONCLUSIONS

Special software based on CUDA parallel computations allowed us to determine the characteristics of helical beams in the accelerated mode in order to evaluate the possibility of using them in laser communica-

tion systems. Our numerical results show that when optimizing systems with helical beam multiplexing, we must consider the variation in the effect misalignment has on beams with different topological charges. At an angle of incidence of one-tenth that of the divergence of the main free space mode, the loss at topological charges varying from 0 to 5 rises from 5 to 20%. Increasing the topological charge influences the effect the inhomogeneity of the propagation medium has on the beam, notably reducing the displacement dispersion of its center of gravity. The random shifts of a helical beam are then inferior to the Gauss mode displacements in the same transverse dimensions. The new way of obtaining tubular helical beams by using powerful multibeam radiation considered in this work is thus an additional tool for notably lengthening the atmospheric tracks of such beams.

FUNDING

This work was supported in part by the Russian Science Foundation, project no. 19-12-00310.

REFERENCES

1. Zotov, A.M., Averchenko, A.V., Korolenko, P.V., and Pavlov, N.N., *Bull. Russ. Acad. Sci.: Phys.*, 2018, vol. 82, no. 1, p. 15.
2. Wang, X., Nie, Z., Liang, Y., et al., *Nanophotonics*, 2018, vol. 7, no. 9, p. 1533.
3. Zhu, F., Huang, S., Shao, W., et al., *Opt. Commun.*, 2017, vol. 396, no. 8, p. 50.
4. Wang, J., *Photonics Res.*, 2016, vol. 4, no. 5, p. 814.
5. Jurado-Navas, A., Tatarczak, A., Lu, X., et al., *Opt. Express*, 2015, vol. 23, no. 26, p. 33721.
6. Aksenov, V.P. and Pogutsa, Ch.E., *Atmos. Oceanic Opt.*, 2013, vol. 26, no. 1, p. 13.
7. Korolenko, P.V., *Optika kogerentnogo izlucheniya* (Coherent Radiation Optics), Moscow: Mosk. Gos. Univ., 1998.
8. Aksenov, V.P., Dudorov, V.V., and Kolosov, V.V., *Quantum Electron.*, 2016, vol. 46, no. 8, p. 726.

Translated by O. Maslova